Signal Decomposition by Using the S-Method With Application to the Analysis of HF Radar Signals in Sea-Clutter

LJubiša Stanković, *Senior Member, IEEE*, Thayananthan Thayaparan, and Miloš Daković

***Abstract*—This paper presents a new approach to the time-frequency signal analysis and synthesis, using the eigenvalue decomposition method. It is based on the S-method, the time-frequency representation that can produce a distribution equal or close to a sum of the Wigner distributions of individual signal components. The new time-frequency signal decomposition method is evaluated on the simulated and experimental high-frequency surface-wave radar (HFSWR) data. Results demonstrate that it provides an effective way for analyzing and detecting maneuvering air targets with significant velocity changes, including target signal separation from the heavy clutter. The analysis shows that this method can provide additional insight into the interpretation and processing of radar signals, with respect to the traditional Fourier transform based methods currently used by the HFSWRs. The proposed method could also be used in other signal processing applications.**

***Index Terms*—Eigenvalues and eigenvectors, high-frequency (HF) radar, radar target recognition, signal decomposition, time-frequency analysis.**

I. Introduction

SIGNALS are commonly analyzed in either time or frequency domain. However, some signals exhibit significant time variations of the frequency content. In these cases, time-frequency representations could be used, since they combine time and frequency domain analyses to yield a more revealing picture of the temporal localization of signals spectral components [5], [14], [22], [23]. The oldest and the most widely used time-frequency representation is the short-time Fourier transform (STFT). In order to improve its concentration, various quadratic representations have been introduced [3], [6], [12]. The most prominent member of this class of representations is the Wigner distribution (WD). Inversion properties of the Wigner distribution and synthesis of a signal from a given time-frequency representation have been studied in [4], [8], [9], [11], and [13].

Manuscript received November 20, 2004; revised November 29, 2005. The associate editor coordinating the review of this manuscript and approving it for publication was Dr. Yuri Abramovich. This work was supported by the Defence Research and Development Canada.

LJ. Stanković and M. Daković are with Elektrotehnički fakultet, University of Montenegro, 81000 Podgorica, Montenegro (e-mail: l.stankovic@ieee.org; milos@cg.ac.yu).

T. Thayaparan is with the Radar Applications and Space Technology, Defence Research and Development Canada, Ottawa, Ontario, Canada (e-mail: Thayananthan.Thayaparan@drdc-rddc.gc.ca).

Digital Object Identifier 10.1109/TSP.2006.880248

The S-method is a time-frequency representation introduced with a goal to be equal (or close) to a sum of the Wigner distributions of individual signal components [17]. It has also been used as a model in the implementation of time-scale representations, time-varying spectra estimation, detection and realization of higher order representations in [2], [10], [15], [16], and [18]. In this paper, the S-method is used to introduce a new method for decomposition of multicomponent signals by using eigenvalues and eigenvectors of an appropriately formed matrix.

The proposed decomposition method is applied in analysis of HFSWR radar signals. Conventionally, targets are detected from radar signals by the Fourier transform or Doppler processing method. However, performance of the Fourier method degrades if the target highly accelerates, resulting in a smeared spectrum. The degree of smearing becomes higher when the number of pulses is increased for a given acceleration or when the acceleration is increased for a given number of pulses [24]. If the smearing is too high, the Fourier method could even fail to detect the target. The case of highly accelerating targets corresponds to the analysis of signals with fast time variations of the frequency content. Therefore, these kinds of signals should be analyzed by the time-frequency representations rather than by the Fourier transform. Time-frequency-based decomposition could also provide extraction of individual signal components. It will be efficient in separating the target signal from an undesirable clutter. This property is of a particular significance in the HFSWR signals where, beside the target signal, there is a clutter that is primarily due to scattering from the surface waves.

The results obtained by applying time-frequency analysis based decomposition method show that one can improve readability performance of the HFSWR, as well as add new insight, over what can be achieved by conventional methods currently used by the HFSWRs.

This paper is organized as follows. After an introduction, inversion of the Wigner distribution is presented in Section II. A review of the S-method definition and its basic properties is given in Section III. This representation is used for defining a new decomposition method of multicomponent signals in Section IV. Next, the signal decomposition is discussed from the point of view of a target signal in a strong sea clutter. Real data analysis, presented in Section V, proves efficiency of the proposed method, and illustrates improvements in readability and detection of the target signal. Finally the Appendix provides a high-resolution form of the S-method.

II. Wigner Distribution Based Inversion and Decomposition

A discrete form of the Wigner distribution is defined by

$$WD(n,k)=\sum_{m=-N/2}^{N/2} f(n+m)f^*(n-m)e^{-j\frac{2\pi}{N+1}2mk} \quad (1)$$

where we assume that the signal $f(n)$ is time limited within $|n|\leq N/2$ and omit a constant multiplication factor of 2. Inversion relation for the Wigner distribution reads

$$f(n+m)f^*(n-m)=\frac{1}{N+1}\times\sum_{k=-N/2}^{N/2}\text{WD}(n,k)e^{j\frac{2\pi}{N+1}m(2k)}.$$

After substitutions $n_1=n+m$ and $n_2=n-m$ we get

$$f(n_1)f^*(n_2)=\frac{1}{N+1}\times\sum_{k=-N/2}^{N/2}\text{WD}\left(\frac{n_1+n_2}{2},k\right)e^{j\frac{2\pi}{N+1}k(n_1-n_2)}. \quad (2)$$

For cases when $(n_1+n_2)/2$ is not an integer, an appropriate interpolation is performed in order to calculate Wigner distribution $\text{WD}((n_1+n_2)/2,k)$.[1] Introducing the notation

$$R(n_1,n_2)=\frac{1}{N+1}\times\sum_{k=-N/2}^{N/2}\text{WD}\left(\frac{n_1+n_2}{2},k\right)e^{j\frac{2\pi}{N+1}k(n_1-n_2)}, \quad (3)$$

we get

$$R(n_1,n_2)=f(n_1)f^*(n_2). \quad (4)$$

Matrix form of (4) reads

$$\mathbf{R}=\mathbf{f}(n)\mathbf{f}^*(n) \quad (5)$$

where $\mathbf{f}(n)$ is a column vector whose elements are the signal values, $\mathbf{f}^*(n)$ is a row vector (Hermitian transpose of $\mathbf{f}(n)$), and $\mathbf{R}$ is a matrix with the elements $R(n_1,n_2)$, defined by (3).

As for any square matrix, the eigenvalue decomposition of $\mathbf{R}$ reads

$$\mathbf{R}=\mathbf{Q}\mathbf{\Lambda}\mathbf{Q}^T=\sum_{i=1}^{N+1}\lambda_i\mathbf{u}_i(n)\mathbf{u}_i^*(n), \quad (6)$$

[1]For better understanding of the calculation procedure note that relation (2) is a discrete counterpart of the Wigner distribution inversion in analog domain, that reads

$$f(t_1)f^*(t_2)=\frac{1}{2\pi}\int_{-\infty}^{\infty}\text{WD}((t_1+t_2)/2,\omega)e^{j\omega(t_1-t_2)}d\omega.$$

By discretizing angular frequency $\omega=k\Delta\omega$ and time $t_1=n_1\Delta t, t_2=n_2\Delta t$, with appropriate definition of discrete values, assuming $\Delta t=1$, we easily obtain (2).

where λ_i are eigenvalues and $\mathbf{u}_i(n)$ are eigenvectors of $\mathbf{R}$. By comparing (5) and (6), it follows that the matrix with elements of form (3) can be decomposed by using only one nonzero eigenvalue. Note that the energy of eigenvectors is equal to 1, by definition $\|\mathbf{u}_1(n)\|^2=1$. By comparing (5) and (6), having in mind that there is only one nonzero eigenvalue, we have $\mathbf{f}(n)\mathbf{f}^*(n)=\lambda_1\mathbf{u}_1(n)\mathbf{u}_1^*(n)=(\sqrt{\lambda_1}\mathbf{u}_1(n))(\sqrt{\lambda_1}\mathbf{u}_1(n))^*$ or

$$\lambda_1=\left\|\sqrt{\lambda_1}\mathbf{u}_1(n)\right\|^2=\|\mathbf{f}(n)\|^2=\sum_{n=-N/2}^{N/2}f^2(n)=E_f$$

resulting in

$$\lambda_i=E_f\delta(i-1) \quad (7)$$

where $\delta(i)$ denotes Kronecker symbol. Eigenvector $\mathbf{u}_1(n)$ is equal to the signal vector $\mathbf{f}(n)$ up to the constant amplitude and phase factor. Therefore, an eigenvalue decomposition of the matrix, formed according to (3), can be used to check if an arbitrary two-dimensional (2-D) function $D(n,k)$ is a valid Wigner distribution.

The same relations can be used in signal synthesis. We start from a given function $D(n,k)$, calculate (3) and perform eigenvalue decomposition (6). The first (largest) eigenvalue and corresponding eigenvector produce a signal such that its Wigner distribution is the closest possible Wigner distribution [in the least-mean-square (LMS) sense] to the given arbitrary function $D(n,k)$, [11].

Now, this property, along with the S-method, will be used for the signal decomposition into its components.

III. S-Method Definition and Basic Property

Note that a definition of the STFT is

$$\text{STFT}(n,k)=\sum_{m=-N/2}^{N/2}f(n+m)e^{-j\frac{2\pi}{N+1}mk}. \quad (8)$$

Its relationship with (1), as derived in [17], is

$$\text{WD}(n,k)=\frac{1}{N+1}\times\sum_{l=-N/2}^{N/2}\text{STFT}(n,k+l)\text{STFT}^*(n,k-l).$$

This relation has led to the S-method definition [17], [21]

$$\text{SM}(n,k)=\frac{1}{N+1}\sum_{l=-L}^{L}\text{STFT}(n,k+l)\text{STFT}^*(n,k-l) \quad (9)$$

or

$$\text{SM}(n,k)=\sum_{l=-N/2}^{N/2}P(l)\text{STFT}(n,k+l)\text{STFT}^*(n,k-l) \quad (10)$$

with the window function $P(l)=1/(N+1)$ for $|l|\leq L$ and $P(l)=0$ elsewhere. The S-method can produce the represen-

tation of a multicomponent signal such that the distribution of each component is its Wigner distribution, avoiding cross-terms.

Proposition: Consider a multicomponent signal

$$f(n)=\sum_{i=1}^{M} f_i(n)$$

where $f_i(n)$ are monocomponent signals. Assume that the STFT of each component lies inside the region $D_i(n,k), i = 1,2,\ldots,M$. Denote the length of ith region along k, for a given n, by $2B_i(n)$, and its central frequency by $k_{0i}(n)$. The S-method of $f(n)$ is equal to the sum of the individual Wigner distributions, $\mathrm{WD}_i(n,k), i = 1,2,\ldots,M$, of each signal's component

$$\mathrm{SM}(n,k)=\sum_{i=1}^{M}\mathrm{WD}_i(n,k) \tag{11}$$

if the regions $D_i(n,k), i = 1,2,\ldots,M$, do not overlap, $D_i(n,k)\cap D_j(n,k)=\emptyset$ for $i\neq j$, and the number of terms L in (9), for a point (n,k), is defined by

$$L(n,k)=\begin{cases} B_i(n)-|k-k_{0i}(n)|, & \text{for } (n,k)\in D_i(n,k)\\ 0, & \text{elsewhere.}\end{cases} \tag{12}$$

Proof is very similar to the one provided for the continuous S-method case. It can be found in [19].

Note 1: Real M-component signals may be considered as $2M$-component complex signals with each region $D_i(n,k)$ being associated with the region $D_{i+M}(n,-k)$. Thus, there is no need for removing negative frequency components in real signals [20].

Note 2: Any window in (9) with a constant number of terms $L \geq \max_{n,k}\{L(n,k)\}$ produces $\mathrm{SM}(n,k) = \sum_{i=1}^{M}\mathrm{WD}_i(n,k)$, if the regions $D_i(n,k), i = 1,2,\ldots,M$, are at least $2L$ apart along the frequency axis, i.e., $|k_{0i}(n) - k_{0j}(n)| > B_i(n) + B_j(n) + 2L$, for each i,j and n.

This is the **S-method with constant value of** L, as it was originally introduced in [17] and [18]. The signal dependent method (12) would be more accurate, but also more complex. Constant number of terms L is used here in numerical realization since it is much simpler for implementation, producing satisfactory and robust results.

IV. Decomposition of Multicomponent Signals

For each signal component $f_i(n)$, we could write its inversion formula, corresponding to (2), as

$$f_i(n_1)f_i^*(n_2)=\frac{1}{N+1}\sum_{k=-N/2}^{N/2}\mathrm{WD}_i\left(\frac{n_1+n_2}{2},k\right)\times e^{j\frac{2\pi}{N+1}k(n_1-n_2)},\quad i=1,2,\ldots,M$$

if we knew the Wigner distribution $\mathrm{WD}_i(n,k)$ of this component. By summing the above relations for $i = 1,2,\ldots,M$, we get

$$\sum_{i=1}^{M} f_i(n_1)f_i^*(n_2)=\frac{1}{N+1}\sum_{k=-N/2}^{N/2}\times\sum_{i=1}^{M}\mathrm{WD}_i\left(\frac{n_1+n_2}{2},k\right)e^{j\frac{2\pi}{N+1}k(n_1-n_2)}.$$

Having in mind (11), for the signals that satisfying the presented conditions, this relation reduces to

$$\sum_{i=1}^{M} f_i(n_1)f_i^*(n_2)=\frac{1}{N+1}\times\sum_{k=-N/2}^{N/2}\mathrm{SM}\left(\frac{n_1+n_2}{2},k\right)e^{j\frac{2\pi}{N+1}k(n_1-n_2)}. \tag{13}$$

By denoting

$$R_{\mathrm{SM}}(n_1,n_2)=\frac{1}{N+1}\sum_{k=-N/2}^{N/2}\mathrm{SM}\left(\frac{n_1+n_2}{2},k\right)\times e^{j\frac{2\pi}{N+1}k(n_1-n_2)} \tag{14}$$

and using the eigenvalue decomposition of matrix $\mathbf{R}_{\mathrm{SM}}$, with the elements $R_{\mathrm{SM}}(n_1,n_2)$, we get

$$\mathbf{R}_{\mathrm{SM}}=\sum_{i=1}^{N+1}\lambda_i\mathbf{u}_i(n)\mathbf{u}_i^*(n).$$

As in the case of Wigner distribution, we can conclude that $\lambda_i = E_{f_i}, i = 1,2,\ldots,M$ and $\lambda_i = 0$ for $i = M+1,\ldots,N$, i.e.,

$$\lambda_i=\sum_{l=1}^{M}E_{f_l}\delta(i-l). \tag{15}$$

The eigenvectors $\mathbf{u}_i(n)$ will be equal to the signal components $\mathbf{f}_i(n)$, up to the phase and amplitude constants, since the components orthogonality is assumed by the Proposition. Amplitude constants are again contained in the eigenvalues λ_i. Thus, the reconstructed signal can be written as

$$f_{\mathrm{rec}}(n)=\sum_{i=1}^{M}\sqrt{\lambda_i}u_i(n).$$

It is equal to the original signal, up to the phase constants in each component. When we have several components of different energies $\mathbf{f}_1(n),\mathbf{f}_2(n),\ldots,\mathbf{f}_M(n)$ and when they are of equal importance in analysis, we can use normalized values of the signal components and calculate the time-frequency representation of

$$\mathbf{f}_{\mathrm{nor}}(n)=\sum_{i=1}^{M}k(\lambda)\mathbf{u}_i(n)$$

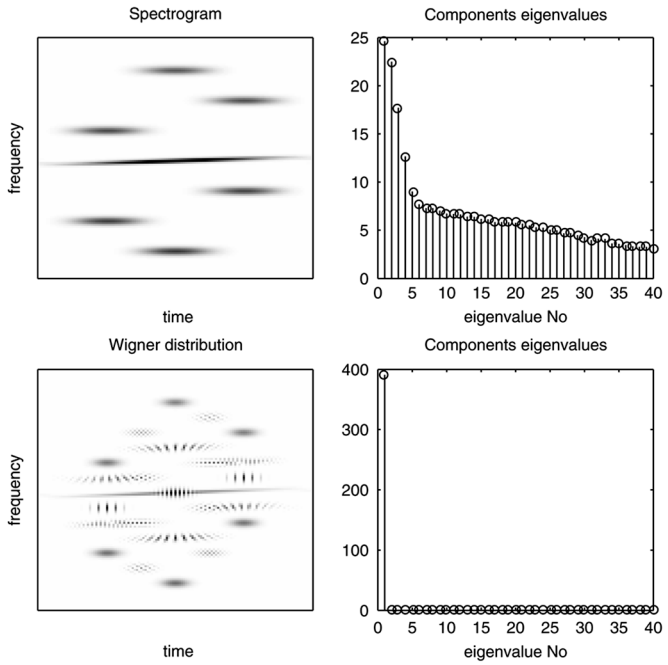

Fig. 1. Spectrogram and its eigenvalue decomposition (upper row); Wigner distribution and its eigenvalue decomposition (bottom row).

by using the weights $k(\lambda) = 1$ in the signal, i.e., by using the eigenvectors as signal components (Capon's way of weighting in the minimal variance high-resolution approach; see the Appendix).

When there exists a very strong disturbing signal, like a sea clutter in the HFSWR signal, we can omit the first, strongest component, and define reconstructed signal as

$$f_{\rm rec}(n) = \sum_{i=2}^{M_1} \sqrt{\lambda_i} u_i(n)$$

where M_1 is the expected number of components.

A. Illustrative Example

Consider a signal whose analog form reads:

$$x(t) = e^{j\frac{\pi}{6400}t^2} e^{-(\frac{t}{96})^2} + \sum_{k=2}^{7} \sqrt{\frac{27-k}{10}} e^{j\omega_k t} e^{-(\frac{t-d_k}{16})^2}$$

within the interval $-128 \leq t \leq 127$, where $\omega_2 = -(3\pi/4), \omega_3 = -(\pi/2), \omega_4 = -(\pi/4), \omega_5 = (\pi/4), \omega_6 = (\pi/2), \omega_7 = (3\pi/4), d_2 = d_7 = 0, d_3 = d_5 = -64$ and $d_4 = d_6 = 64$. The sampling interval is $\Delta t = 1$. Spectrogram, calculated according to (8), is presented in Fig. 1, upper row. The Wigner distribution is presented in Fig. 1, bottom row. Based on the Wigner distribution, the elements of matrix $\mathbf{R}$ are calculated by using (3). Eigenvalue decomposition (6) of this matrix produces exactly one nonzero eigenvalue, $\lambda_1 = 390.92 (\lambda_2 = 0.00, \lambda_3 = 0.00, \cdots)$, being equal to the total signal energy $E_x = 390.14$ (within the numerical calculation error), as expected from (3)–(7).

In order to illustrate that eigenvalue decomposition of the spectrogram (that is the first step in S-method calculation) does not produce a meaningful result, we have repeated this procedure by using the spectrogram instead of the Wigner distribution in the calculation of the elements of $\mathbf{R}$, according to (3). The eigenvalue decomposition obtained in this way proves that the spectrogram can not be related to a sum of the Wigner distributions of the signal components [Fig. 1, upper row (right)].

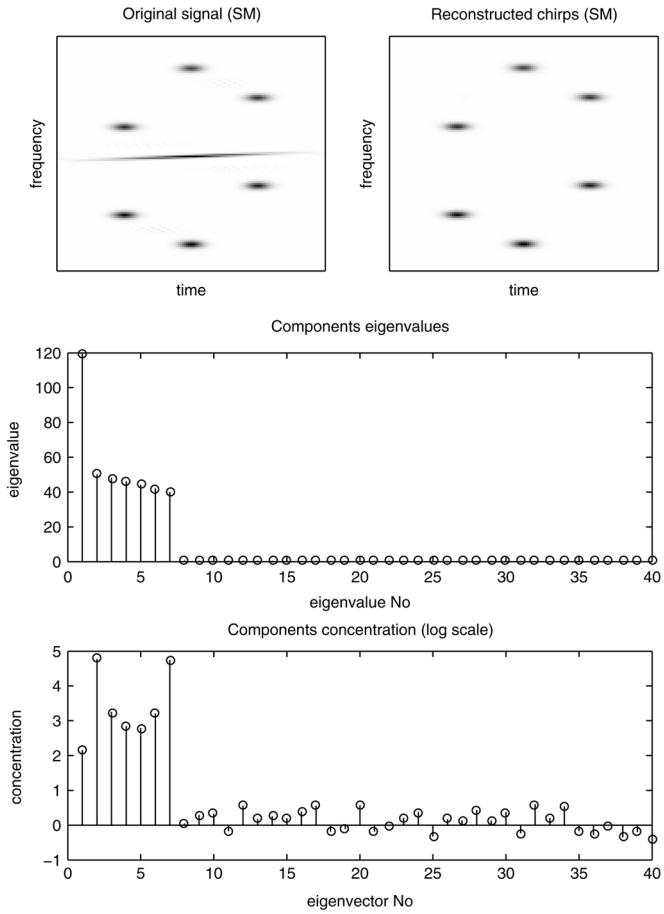

Fig. 2. S-method of original multicomponent signal (first row, left); the S-method of reconstructed signal by using eigenvectors, with omitted first eigenvector-component (first row right); eigenvalues of the signal's S-method; measure of concentration of signal components (eigenvectors) in logarithmic scale.

The S-method of the same signal is calculated by using (8) and (9) with $L = 12$. The obtained results are depicted in Fig. 2. Matrix $\mathbf{R}_{\rm SM}$ is formed according to (14). Its eigenvalue decomposition results in the same number of nonzero eigenvalues as the number of signal components. Eigenvalues correspond to the components energies, while the eigenvectors correspond to the normalized signal components, up to the phase constants. Time-frequency representation of the eigenvectors is shown in Fig. 3. First seven components correspond to the signal, while the remaining ones are with very small eigenvalues. Energies of discrete signal components are: $E_1 = 119.40, E_2 = 50.13, E_3 = 48.13, E_4 = 46.12, E_5 = 44.12, E_6 = 42.11$ and $E_7 = 40.11$, while the obtained eigenvalues by using the S-method with $L = 12$ are: $\lambda_1 = 119.40, \lambda_2 = 50.18, \lambda_3 = 48.19, \lambda_4 = 46.19, \lambda_5 = 44.18, \lambda_6 = 42.17, \lambda_7 = 40.15, \lambda_8 = 0.68, \cdots$.

Sensitivity of the results with respect to L is quite low within a wide region. We have repeated calculations with values of L

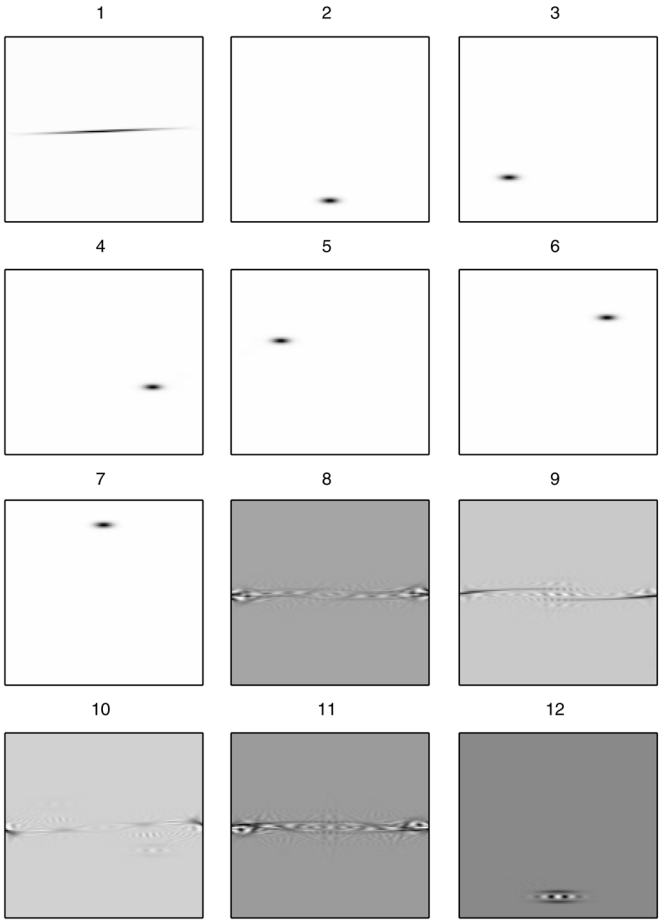

Fig. 3. Time-frequency representation of the eigenvectors of the S-method. First seven of them correspond to the normalized signal components. In all subplots, horizontal axis is for time and vertical axis is for frequency.

from $L = 10$ up to $L = 20$ and obtained almost the same results. The error in components energy, estimated by corresponding eigenvalues, was within $\pm 0.25\%$.

As a decomposition example, we omitted the strongest component and reconstructed the rest of the signal. The obtained time-frequency representation is given in the upper row (right) of Fig. 2. The last subplot in Fig. 2 presents concentration measure of the components, in logarithmic scale, which will be discussed and used later.

B. Decomposing Radar Time-Varying Signals in a Strong Sea-Clutter

Next we will apply the proposed method to the HFSWR signals with a strong sea clutter. Before we start analysis of experimental data, we will consider some typical situations from the theoretical point of view.

1) When the sea-clutter signal and the target signal are separated in time-frequency plane (occupying unknown and varying ranges in time-frequency domain) and at the same time, the signal energy is of the clutter energy order, it will be possible to get a decomposition such that the first component corresponds to the stronger clutter and the second component corresponds to the target signal. In this case

$$\mathbf{u}_1(n) \sim \mathbf{f}_{\text{clutter}}(n) = \sqrt{\lambda_1} e^{j\varphi_1} \mathbf{u}_1(n)$$
$$\mathbf{u}_2(n) \sim \mathbf{f}_{\text{target}}(n) = \sqrt{\lambda_2} e^{j\varphi_2} \mathbf{u}_2(n)$$

where φ_1 and φ_2 are arbitrary phase constants. Separate time-frequency representation of the clutter and target signal would be easy in this case.
2) Now consider the case when target signal is much weaker than the sea-clutter signal and the value of L is not sufficiently large to complete the integration over clutter and target signal, according to (12). Then, the first several components can be attributed to the clutter signal only (smaller L will increase the number of clutter components). The main part of the clutter and the residual clutter parts are stronger than the target signal. Here, we have to define a criterion to select and resolve the target signal component.
3) The sea-clutter signal and the target signal are close or crossing each other or target signal is highly nonstationary covering wide area. In this case, both the clutter and the signal could be separated into few parts, and the criterion for selecting the target components should be defined, as well.

C. Criterion for Identifying Target Components

Note that the signal components in HFSWR are single frequency modulated signals, better concentrated in the time frequency plane than the clutter residual components. Thus, the criterion for selecting eigenvector(s), being the target signal (or parts of the target signal), could be

$$C_{\text{rit}}(p) = \frac{(N+1)\max_{n,k}\{\text{SM}_{u_p}(n,k)\}}{\sum_{k=-N/2}^{N/2}\sum_{n=-N/2}^{N/2}\left|\text{SM}_{u_p}(n,k)\right|}$$

or

$$C^{-}_{\text{rit}}(p) = \frac{(N+1)\max_{n,k}\{\text{SM}_{u_p}(n,k)\}}{2\sum_{k=-N/2}^{N/2}\sum_{n=-N/2}^{N/2}\left|\text{SM}^{-}_{u_p}(n,k)\right|} \quad (16)$$

where $\text{SM}^{-}_{u_p}(n,k)$ denotes negative values of $\text{SM}_{u_p}(n,k)$. It means that higher concentrated components (greater maximum in the numerator, since all eigenvectors are normalized in energy) with smaller oscillations (smaller mean absolute (negative) value in the denominator) are better candidates for the target signal components. This criterion can be considered as concentration measure, with infinity power in the numerator and power 1 in the denominator of $C_{\text{rit}}(p)$. It can also be understood as the peak-to-average absolute value ratio.

The simplest algorithm is to find the value when $C_{\text{rit}}(p)$ reaches maximal value ($p = p_{\max}$) and assign this eigenvector to the target signal component:

$$\mathbf{f}_{\text{target}}(n) = \mathbf{u}_{p_{\max}}(n).$$

This simple approach works well in most of the considered signals. Of course, the strongest component in decomposition is the clutter, thus $\mathbf{u}_1(n)$ is omitted from the analysis.

For few considered signals, the target signal component is divided over several eigenvectors, as discussed in cases 2 and 3 mentioned within the previous subsection. In order to deal with these cases, let us analyze the range for $C_{\rm rit}(p)$ values. If the whole distribution of one component is concentrated at one point in time-frequency plane, i.e., $\mathrm{SM}_{u_p}(n,k) = A\delta(n-n_0, k-k_0)$, then $C_{\rm rit}(p) = N+1$. For a component that is uniformly distributed along a single line, i.e., pure linear frequency modulated component, $C_{\rm rit}(p) = 1$. For uniformly spread distribution values over the entire time-frequency plane (obviously not being a signal component), we have $C_{\rm rit}(p) = 1/(N+1)$. Thus, we can say that if, for example $C_{\rm rit}(i) > P$, where P is of order 1 or just slightly higher, for $i = k, p, \ldots, q$, then $\mathbf{u}_i(n)$ are parts of the target signal, i.e.,

$$H(i) = \begin{cases} C_{\rm rit}(i) > P, & \mathbf{u}_i(n) \text{ is a target signal component} \\ C_{\rm rit}(i) \le P, & \mathbf{u}_i(n) \text{ is not a target signal component} \end{cases}.$$

Thus, we can take all eigenvectors that satisfy this criterion and form the target signal

$$\mathbf{f}_{\rm target}(n) = \sqrt{\lambda_k}\mathbf{u}_k(n) + \sqrt{\lambda_p}\mathbf{u}_p(n) + \cdots + \sqrt{\lambda_q}\mathbf{u}_q(n) \tag{17}$$

with $i = k, p, \ldots, q$ and $i > 1$, since the first component will always be the strongest one corresponding to the clutter. Note that if L in (9) is not large enough to complete the integration over the clutter, then few of the largest components will be ones belonging to the clutter and $i > 2$ components should be omitted.

In the time-frequency domain, we get

$$\begin{aligned}\mathrm{SM}_{\rm target}(n,k) &= g(\lambda_k)\mathrm{SM}_k(n,k) \\ &\quad + g(\lambda_p)\mathrm{SM}_p(n,k) + \cdots + g(\lambda_q)\mathrm{SM}_q(n,k)\end{aligned} \tag{18}$$

where $g(\lambda)$ is a function of eigenvalue. If we want to take all the components with the same weight $g(\lambda) = 1$, or if we want to keep their original weights $g(\lambda) = \lambda$. Cases between these two are possible, for example $g(\lambda) = \sqrt{\lambda}$.

D. Numerical Realization

Numerical realization of the S-method (9),(12) is very simple, according to

$$\mathrm{STFT}(n,k) = \mathrm{DFT}_m\{x(n+m)w(m)\}$$

and

$$\begin{aligned}\mathrm{SM}(n,k) &= |\mathrm{STFT}(n,k)|^2 \\ &\quad + 2\sum_{i=1}^{L} \Re[\mathrm{STFT}(n,k+i)\mathrm{STFT}^*(n,k-i)]\end{aligned}$$

or

$$\begin{aligned}\mathrm{SM}_L(n,k) &= \mathrm{SM}_{L-1}(n,k) \\ &\quad + 2\Re[\mathrm{STFT}(n,k+L)\mathrm{STFT}^*(n,k-L)]\end{aligned} \tag{19}$$

where $\mathrm{SM}_L(n,k)$ is $\mathrm{SM}(n,k)$ calculated with L samples in (9) and $\mathrm{SM}_0(n,k) = \mathrm{SPEC}(n,k) = |\mathrm{STFT}(n,k)|^2$. Symbol $\Re[\cdot]$ stands for real value.

Calculation complexity: The basic step in the S-method realization is in calculation of the STFT by using the fast Fourier transform (FFT) algorithms or recursive formulas [17]. Calculation of the STFT in M time instants by using the N samples FFT requires an $MN\log_2 N$ order of basic arithmetic operations (multiplications and additions). The additional block for the S-method calculation, according to (19), requires MNL arithmetic operations. For example, for $N = 1024$ and $L = 10$, the additional number of arithmetic operations is of the same order as the basic STFT calculation. It is significantly less intensive than the calculation of Wigner distribution or any other quadratic representation [17]. In addition, the S-method can be implemented in hardware [21], which makes the calculation complexity problem less important. Furthermore, the coherent integration time in the considered example is quite long. Decomposition of the S-method based matrix is done by using the standard iterative eigenvalue decomposition procedures, with a given number of significant eigenvalues (we used 36 significant eigenvalues). We checked the calculation time in MATLAB algorithms. The eigenvalue decomposition increased this time for 29% of the time required for the calculation of the STFT and the S-method with $L = 10, N = 1024$ and $M = 512$.

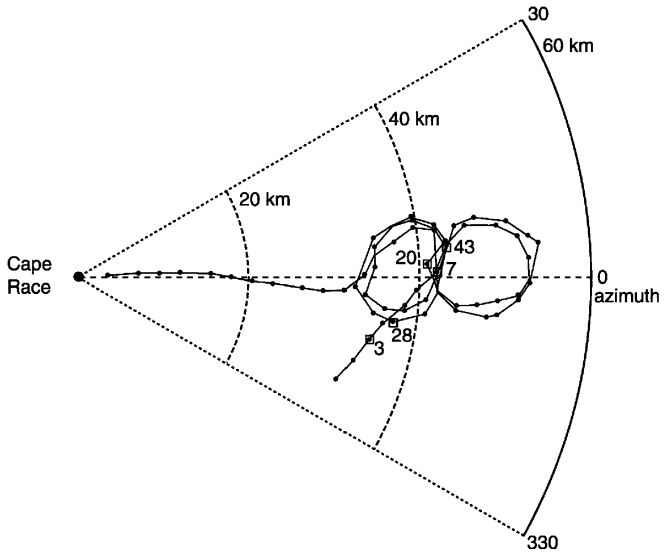

Fig. 4. Path of the King-Air 200 as a function of range (in km) and azimuth (in degrees).

V. Data Analysis

The signals considered here are experimental plane data, as used in [22]. The plane is a King-Air 200 performing maneuvers, tracked by a HFSWR, using a ten-element linear receiving antenna array. The radar carrier frequency is 5.672 MHz and the pulse repetition frequency is 9.17762 Hz. Each trial corresponds to a block of 256 pulses. Therefore, the CIT (coherent integration time) of each signal is 27.89 sec. The King-Air performed two figure-of-eight maneuvers (Fig. 4). Each figure-of-eight maneuver consisted of two circles with an approximate diameter of 10 km. The first figure-of eight maneuver was performed at 200 ft (61 m), while the second figure-of-eight maneuver was performed at 500 ft (152 m). The location of the King-Air, when each signal was collected, is marked by a square (Fig. 4). Each signal reflects a different scenario that could arise when tracking the maneuvering plane.

In the HFSWR, beside the target, signal contain a clutter that is primarily due to scattering from the surface of sea waves. The received signal of a pulse Doppler radar, taken at a particular range, is viewed in the Fourier transform or Doppler domain. Two sharp peaks, Bragg components, can be observed. These peaks mean that the dominant form of sea clutter is due to scattering from sea waves, with wavelengths being half of the wavelength of the radar carrier frequency, travelling radially towards and away from the radar [7], [1]. The Bragg components of the clutter are called 1st order clutter. In addition to the Bragg components, the Doppler spectrum has a continuum called the second-order clutter.

A. Calculation Procedure

Denote signal length by N. In all considered cases, we use $N = 256$.

Step 1) Calculate the STFT (with rectangular window) of the zero-padded signal, oversampled by factor 2.

Step 2) Calculate the S-method of the signal according to (19) for a given L, for example $L = 10$. Size of obtained S-method is $2N = 512$ samples in time and $4N = 1024$ samples in frequency. Central part of the S-method in frequency domain is equivalent to the Wigner distribution. Note that the frequency range of the S-method is like in the Fourier transform $(-f_s/2, f_s/2)$ and $(-f_s/4, f_s/4)$ for the Wigner distribution, where f_s is the sampling frequency. Only even samples are included in further analysis in order to avoid noninteger indices in (14).

Step 3) Calculate matrix $\mathbf{R}$ according to (14). Since the signal is zero-padded, use only even rows in order to avoid noninteger indices. Since only central part of S-method, and only even samples are used, order of the matrix $\mathbf{R}$ is $N = 256$.

Step 4) Decompose $\mathbf{R}$ into eigenvectors and eigenvalues. Note that eigenvectors has the same length as the original signal.

Step 5) Calculate the S-method (19) of the eigenvectors by using the STFT with a window, for example square root Hann window of 256 samples.

Step 6) Calculate measure (16) and assign the eigenvector corresponding to the maximal measure to the target signal if $C^{-}_{\mathrm{rit}}(p_{\max}) > 2$. If $C^{-}_{\mathrm{rit}}(p_{\max}) \leq 2$ then there is no target signal detected (target signal is too close to the clutter). In this case, repeat Steps 1) to 6) with smaller L, for example $L = 4$. If $C^{-}_{\mathrm{rit}}(p_{\max}) > 2$ check if there is any other highly concentrated eigenvector, for example with $C^{-}_{\mathrm{rit}}(p \neq p_{\max}) > 3$. If there is such a highly concentrated eigenvector, it should also be a part of the target signal. Include it according to (17).

Step 7) Show time-frequency representation of the resulting target signal (23) and calculate its high-resolution version (24), with excluded isolated points. High-resolution images are obtained by using the high-resolution version of the S-method presented in the Appendix. After a high-resolution distribution is calculated, the pattern recognition algorithm is used to eliminate instants when isolated points are produced (random maxima at the instants when there is no target signal component). Only those regions where more than ten connected points of the high-resolution S-method exist are kept for final high-resolution presentation.

Step 8) Take the next signal and go to Step 1).

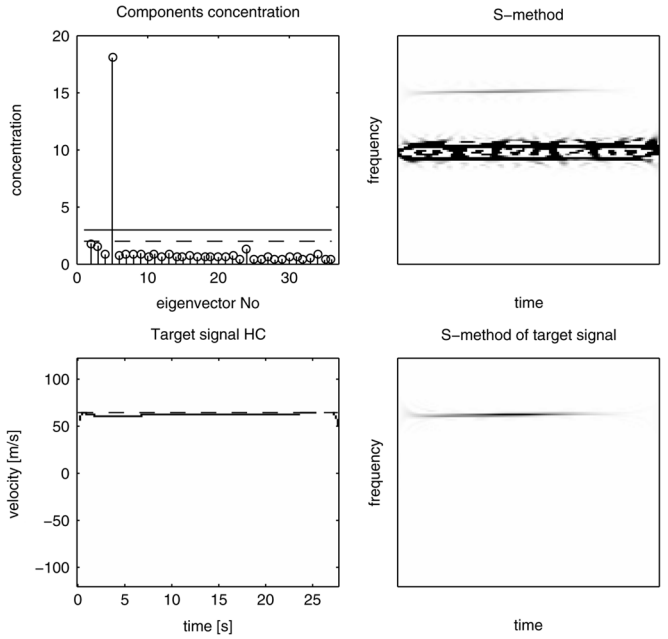

Fig. 5. Signal 3 (reference to Fig. 4.): time-frequency representation (top right), concentration of the eigenvectors time-frequency representations (top left), time-frequency representation of the detected target signal (bottom right), highly concentrated time-frequency representation of the detected target signal (bottom left), and FFT estimation of the target velocity (dashed line).

By using this procedure we analyzed all positions for the described experiment. The target signal is detected and separated in all cases. In four cases, the target signal was too close to the clutter, and the target was not detected with $L = 10$. The procedure was repeated with $L = 4$, according to the description in Step 6), and the target was then detected.

B. Results

Now, the proposed procedure is applied to the signal decomposition. The following are typical cases:

— stationary target signal (plane is moving with a constant velocity), far from the clutter (Fig. 5); the time-frequency representation of the corresponding eigenvectors is shown in Fig. 6;

— nonstationary target signals far from the clutter (Figs. 7 and 9) along with time-frequency representation of the eigenvectors (Fig. 8) for the signal shown in Fig. 7;

— highly nonstationary target signal covering wide frequency range (Fig. 10);

— nonstationary target signal very close to the clutter (Fig. 11);

— nonstationary target signal crossing the clutter (Fig. 12).

For all the signals, the time-frequency representation (S-method) of the original signal including the clutter, is given (upper right subplot in Figs. 5, 7, and 9–12). Since the clutter

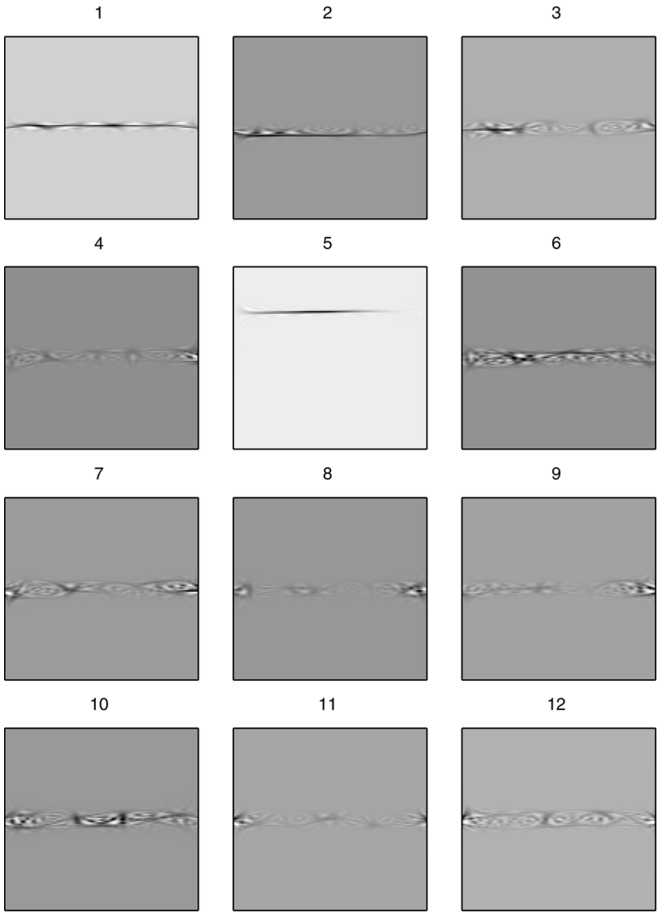

Fig. 6. Time-frequency representations of the eigenvectors used for the concentration calculation and target signal detection for signal presented in Fig. 5. In all subplots, horizontal axis is for time, and vertical axis is for frequency.

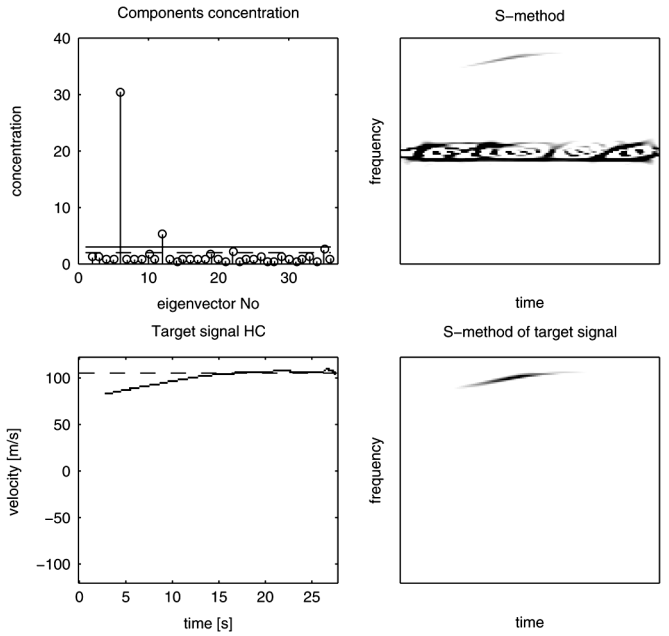

Fig. 7. Signal 31: Time-frequency representation (top right), concentration of the eigenvectors time-frequency representations (top left), time-frequency representation of the detected target signal (bottom right), highly concentrated time-frequency representation of the detected target signal (bottom left), and FFT estimation of the target velocity (dashed line).

is extremely strong, in order to get signal component visible, *the limiter is used in time-frequency representation*. Upper left subplot represents concentration measure for eigenvectors in all considered cases. Lower subplots present S-method of the detected target signal component (right) and its highly concentrated version (left). Frequency axis in the highly concentrated representations is scaled to represent target instantaneous radial velocity while dashed line represents target radial velocity obtained by standard FFT technique. Figs. 6 and 8 present time-frequency representations of the eigenvectors used for the concentration measure and target signal component detection.

For comparison with the FFT method, we will present three cases: nonaccelerating target far from the Bragg's lines, accelerating target far from the Bragg's lines and the target very close to the Bragg's lines (Fig. 13). As expected, in the case of constant velocity (nonaccelerating target) the FFT method produces a clear result with a peak corresponding to the Doppler frequency. It is in accordance and in good agreement with the time-frequency result presented in Fig. 5. However, in the second case the FFT method is smeared, and the constant frequency estimated based on the FFT does not correspond to the real event of fast varying target velocity (Fig. 10). In the third case, there is a slightly smeared peak, but connected to the clutter spectrum. Considering only the FFT it would be difficult to conclude that the target exists. Time-frequency-based approach clearly indicates that we have a target signal, including its separation by the proposed method (Fig. 11). Note that the velocities obtained by using the FFT approach are presented for all considered cases, as mentioned earlier.

VI. Conclusion

We proposed a new time-frequency based signal decomposition method. It is based on the property that the eigenvalue decomposition of an appropriately formed matrix of the Wigner distribution produces only one nonzero eigenvalue, combined with the property that the S-method can produce a sum of the Wigner distributions of individual signal components. Efficiency and accuracy of the proposed decomposition method is demonstrated on simulated examples. Then, it is used in improving the analysis of signals obtained from a low-altitude aircraft by using the HFSWR in the presence of sea clutter. Since we were dealing with high speeds and accelerations of the aircraft, the time-frequency method improved readability and detection, because its resolution abilities were not reduced by a spread in the Doppler signature. The study performed by using the new method demonstrated that use of time-frequency signal decomposition can improve target velocity estimation and detection performance of the HFSWR. The method provided true time varying Doppler shift within the considered time, which was not possible with the Fourier transform method that provided only its average value. In addition, the proposed method successfully detected the target signal in all cases of the presented real experiment, which was not the case when detection was performed by the Fourier transform method. The method presented here is not restricted to this application, but it can be applied also in various other settings of nonstationary signal analysis and filtering.

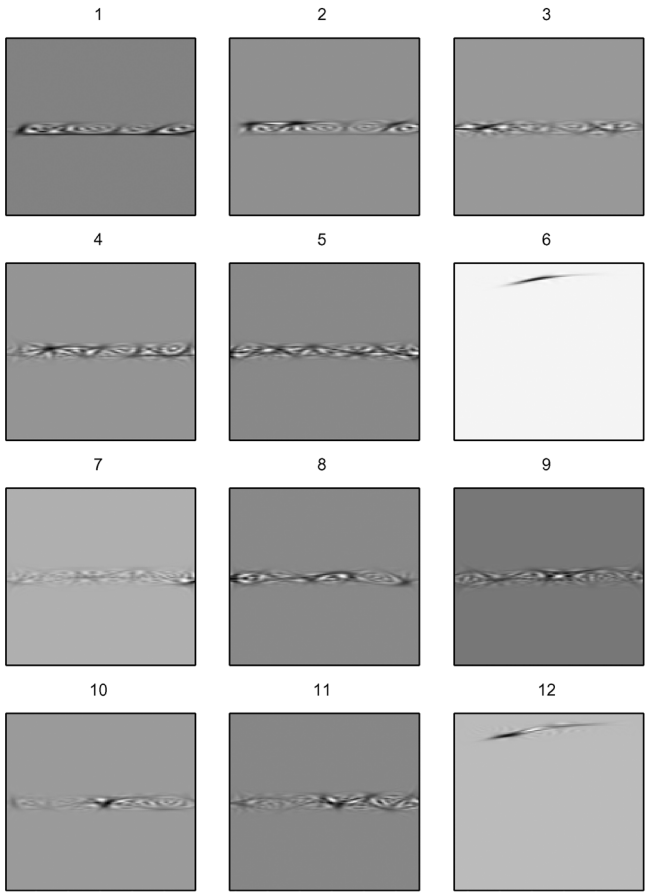

Fig. 8. Time-frequency representations of the eigenvectors used for the concentration calculation and target signal detection for signal presented in Fig. 7. In all subplots, the horizontal axis is for time, and the vertical axis is for frequency.

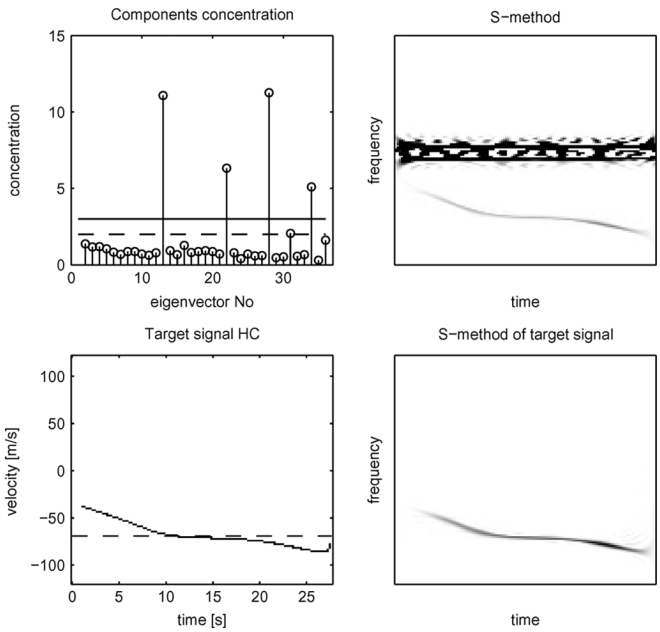

Fig. 9. Signal 43: Time-frequency representation (top right), concentration of the eigenvectors time-frequency representations (top left), time-frequency representation of the detected target signal (bottom right), highly concentrated time-frequency representation of the detected target signal (bottom left), and FFT estimation of the target velocity (dashed line).

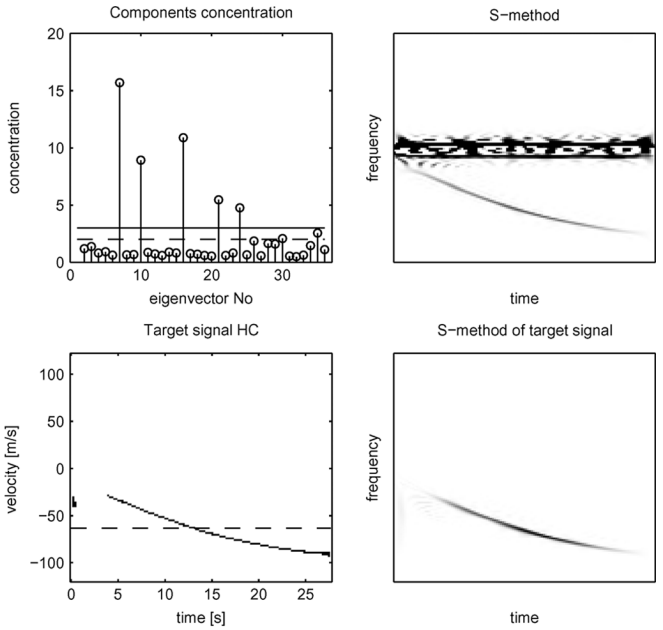

Fig. 10. Signal 53: Time-frequency representation (top right), concentration of the eigenvectors time-frequency representations (top left), time-frequency representation of the detected target signal (bottom right), highly concentrated time-frequency representation of the detected target signal (bottom left), and FFT estimation of the target velocity (dashed line).

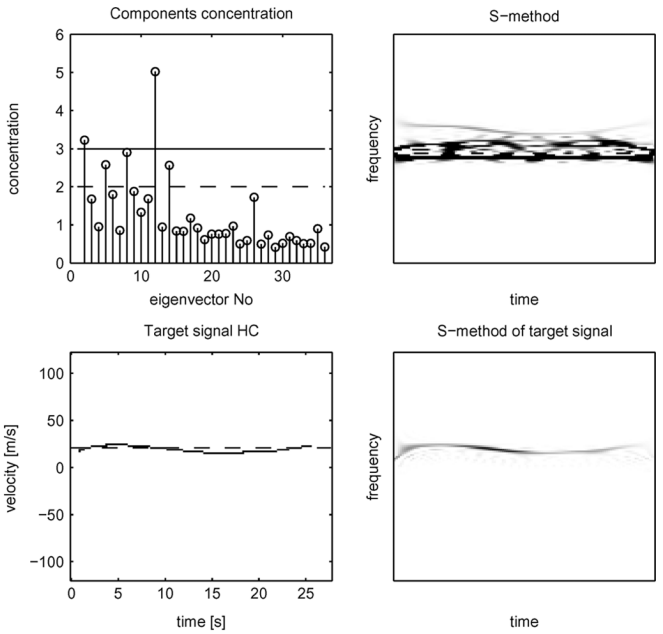

Fig. 11. Signal 7: Time-frequency representation (top right), concentration of the eigenvectors time-frequency representations (top left), time-frequency representation of the detected target signal (bottom right), highly concentrated time-frequency representation of the detected target signal (bottom left), and FFT estimation of the target velocity (dashed line).

APPENDIX
HIGH RESOLUTION S-METHOD WITH RELATION TO THE CAPON'S METHOD

As shown in [16], all spectral estimators can be considered as either being smoothed or being cross-calculated. The first family leads to the variations of smoothed spectrograms, while the other leads to the variations of the estimators defined in [17]. Here, we will show that the Capon's method can be considered

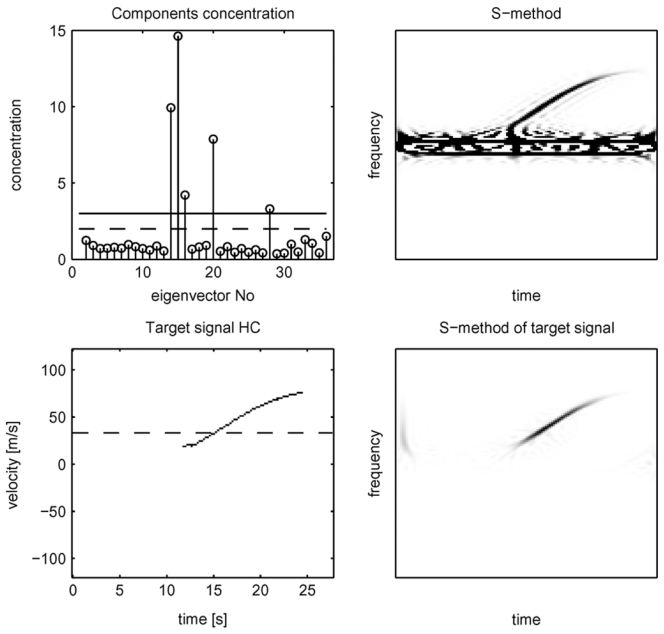

Fig. 12. Signal 19: Time-frequency representation (top right), concentration of the eigenvectors time-frequency representations (top left), time-frequency representation of the detected target signal (bottom right), highly concentrated time-frequency representation of the detected target signal (bottom left), and FFT estimation of the target velocity (dashed line).

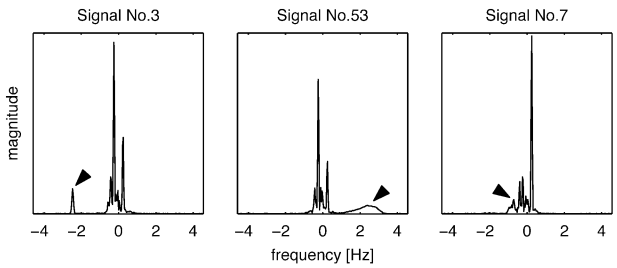

Fig. 13. Fourier transform (absolute value) of the three typical signals: nonaccelerating target far from Bragg's lines, accelerating target far from Bragg's lines and target very close to Bragg's lines. Triangle arrows show target signal.

as a version of the smoothed spectrograms (spectrograms of eigenvectors for close signal components and spectrograms of signal components for separated components). A form of highly concentrated distributions based on the S-method may be defined in an analogous manner, using the analysis presented in this paper.

The Capon's filtering method applied to $N+1$ samples of a signal $f(n)$, being a sum of complex sinusoids $\exp(j\omega_i n)$, denoted in a vector form as $\mathbf{f}(n)$ results in the distribution

$$S_{\text{Cap}}(n,k) = \frac{1}{\mathbf{a}^*(k)\hat{\mathbf{R}}_{\mathbf{f}}^{-1}\mathbf{a}(k)} \tag{20}$$

where * denotes Hermitian transpose and $\mathbf{a}(k) = [1, e^{j2\pi k/(N+1)}, \ldots, e^{j2\pi k}]^T$, with

$$\hat{\mathbf{R}}_{\mathbf{f}} = E\{\mathbf{f}(n)\mathbf{f}^*(n)\}. \tag{21}$$

In practice, the autocorrelation matrix $\hat{\mathbf{R}}_{\mathbf{f}}$ is estimated by

$$\begin{aligned}\hat{\mathbf{R}}_{\mathbf{f}}(n,K) &= \frac{1}{K}\sum_{p=1}^{K}\mathbf{f}(n+p)\mathbf{f}^*(n+p) + \rho\mathbf{I} \\ &= \frac{1}{K}\mathbf{Q}\mathbf{Q}^* + \rho\mathbf{I}\end{aligned} \tag{22}$$

where $\mathbf{I}$ is the identity matrix used for regularization and $\mathbf{Q}$ is the matrix whose columns are signal vectors $\mathbf{f}(n+p), p = 1, \ldots, K$.

The Capon's form can be written by using eigenvalue decomposition of the autocorrelation matrix $\hat{\mathbf{R}}_{\mathbf{f}}(n,K)$ as

$$\hat{\mathbf{R}}_{\mathbf{f}}(n,K) = \frac{1}{K}\mathbf{Q}\mathbf{Q}^* + \rho\mathbf{I} = \frac{1}{K}\mathbf{V}\mathbf{\Lambda}\mathbf{V}^* + \rho\mathbf{I}.$$

By using this decomposition, we can write

$$\hat{\mathbf{R}}_{\mathbf{f}}^{-1}(n,K) = \frac{1}{\rho}\left[\mathbf{I} - \sum_{p=1}^{K}\left(1+\frac{\rho K}{\lambda_p}\right)^{-1}\mathbf{V}_p\mathbf{V}_p^*\right]$$

where $\mathbf{V}_p$ are eigenvectors and λ_p are eigenvalues of $\hat{\mathbf{R}}_{\mathbf{f}}(n,K)$ The Capon's form then reads

$$S_{\text{Cap}K}(n,k) = \frac{\rho}{N+1-\sum_{p=1}^{K}\frac{\lambda_p}{K\rho+\lambda_p}\text{SPEC}_{V_p}(n,k)}$$

where $\text{SPEC}_{V_p}(\omega,t)$ are the spectrograms of the eigenvectors and $\rho \to 0$. *For separated components the eigenvectors correspond to the signal components, summed with the same weights.*

In our case, the S-method form that corresponds to the Capon's form would lead to the factor of

$$\text{SM}_{\text{nor}}(n,k) = \sum_{p=1}^{K}\text{SM}_{u_p}(n,k)$$

instead of $\sum_{p=1}^{K}\text{SPEC}_{V_p}(n,k)$ in the Capon's form, resulting in a distribution

$$\begin{aligned}\text{SM}_{\text{CK}}(n,k) &= \frac{\rho}{N+1-\sum_{p=1}^{K}\rho_p\text{SM}_{u_p}(n,k)} \\ &= \frac{A}{1-\sum_{p=1}^{K}c_p\text{SM}_{u_p}(n,k)}\end{aligned} \tag{23}$$

where $A = \rho/(N+1)$ and $c_p = \rho_p/(N+1)$.

In the realization we used a very simple normalized version of the highly concentrated S-method:

$$\text{SM}_{CK}(n,k) = \frac{1}{1-\sum_{p=1}^{K}\frac{\text{SM}_{u_p}(n,k)}{1.01\max_k\{\text{SM}_{u_p}(n,k)\}}}. \tag{24}$$

REFERENCES

[1] D. Barrick, "First-order theory and analysis of MF/HF/VHF scatter from the sea," *IEEE Trans. Antennas Propag.*, vol. 20, no. 1, pp. 2–10, Jan. 1972.

[2] B. Boashash and B. Ristic, "Polynomial time-frequency distributions and time-varying higher order spectra: Applications to analysis of multicomponent FM signals and to treatment of multiplicative noise," *Signal Process.*, vol. 67, no. 1, pp. 1–23, May 1998.

[3] B. Boashash, Ed., *Time-Frequency Signal Anlysis and Processing*. New York: Elsevier, 2003.

[4] G. F. Bourdeaux-Bartels, "Time-varying signal processing using Wigner distribution synthesis techniques," in *The Wigner Distribution-Theory and Applications in Signal Processing*, W. Mecklenbrauker, Ed. Amsterdam, The Netherlands: Elsevier, 1997.

[5] V. C. Chen and H. Ling, *Time-Frequency Transforms for Radar Imaging and Signal Analysis*. Boston, MA, USA: Artech House, 2002.

[6] L. Cohen, *Time-Frequency Analysis*. Englewood Cliffs, NJ: Prentice-Hall, 1995.

[7] D. D. Crombie, "Doppler spectrum of sea echo at 13.56 Mc/s," *Nature*, no. 175, pp. 681–682, 1955.

[8] G. S. Cunningham and W. J. Williams, "Vector-valued time-frequency representations," *IEEE Trans. Signal Process.*, vol. 44, no. 7, pp. 1642–1656, Jul. 1996.

[9] A. Francos and M. Porat, "Analysis and synthesis of multicomponent signals using positive time-frequency distributions," *IEEE Trans. Signal Process.*, vol. 47, no. 2, pp. 493–504, Feb. 1999.

[10] P. Goncalves and R. G. Baraniuk, "Pseudo affine Wigner distributions: definition and kernel formulation," *IEEE Trans. Signal Process.*, vol. 46, no. 6, pp. 1505–1516, Jun. 1998.

[11] F. Hlawatsch and W. Krattenthaler, "Bilinear signal synthesis," *IEEE Trans. Signal Process.*, vol. 40, no. 2, pp. 352–363, Feb. 1992.

[12] J. Jeong and W. J. Williams, "Kernel design for reduced interference distributions," *IEEE Trans. Signal Process.*, vol. 40, no. 2, pp. 402–412, Feb. 1992.

[13] W. Mu, M. G. Amin, and Y. Zhang, "Bilinear signal synthesis in array processing," *IEEE Trans. Signal Process.*, vol. 51, no. 1, pp. 90–100, Jan. 2003.

[14] S. Qian and D. Chen, *Joint Time-Frequency Analysis: Methods and Applications*. Englewoods Cliffs, NJ: Prentice-Hall, 1996.

[15] C. Richard, "Time-frequency-based detection using discrete-time discrete-frequency Wigner distributions," *IEEE Trans. Signal Process.*, vol. 50, no. 9, pp. 2170–2176, Sep. 2002.

[16] L. L. Scharf and B. Friedlander, "Toeplitz and Hankel kernels for estimating time-varying spectra of discrete-time random processes," *IEEE Trans. Signal Process.*, vol. 49, no. 1, pp. 179–189, Jan. 2001.

[17] L. J. Stanković, "A method for time-frequency analysis," *IEEE Trans. Signal Process.*, vol. 42, no. 1, pp. 225–229, Jan. 1994.

[18] L. J. Stanković, "An analysis of some time-frequency and time-scale distributions," *Annales Telecommun.*, pp. 505–517, Sept./Oct. 1994.

[19] L. J. Stanković and J. F. Böhme, "Time-frequency analysis of multiple resonances in combustion engine signals," *Signal Process.*, vol. 79, no. 1, pp. 15–28, Nov. 1999.

[20] L. J. Stanković and I. Djurović, "A note on 'An overview of aliasing errors in discrete-time formulations of time-frequency representations'," *IEEE Trans. Signal Process.*, vol. 49, no. 1, pp. 257–259, Jan. 2001.

[21] S. Stanković and L. J. Stanković, "An architecture for the realization of a system for time-frequency analysis," *IEEE Trans. Circuits Syst. II, Analog Digit. Signal Process.*, vol. 44, pp. 600–604, Jul. 1997.

[22] T. Thayaparan and S. Kennedy, "Detection of a manoeuvring air target in sea-clutter using joint time-frequency analysis techniques," *Proc. Inst. Elect. Eng.—Radar Sonar Navig.*, vol. 151, no. 1, pp. 19–30, Feb. 2004.

[23] T. Thayaparan, G. Lampropoulos, S. K. Wong, and E. Riseborough, *Focusing ISAR Images Using Adaptive Joint Time-Frequency Algorithm on Simulated and Experimental Radar Data*. Ottawa, ON, Canada: Defence R&D, 2003, TM 2003-089.

[24] A. Yasotharan and T. Thayaparan, "Strengths and limitations of the Fourier method for detecting accelerating targets by pulse Doppler radar," *Proc. Inst. Elect. Eng.—Radar, Sonar, Navig.*, vol. 149, no. 2, pp. 83–88.

LJubiša Stanković (M'91–SM'96) was born in Montenegro on June 1, 1960. He received the B.S. degree from the University of Montenegro, Podgorica, in 1982, the M.S. degree from the University of Belgrade, Belgrade, Yugoslavia, in 1984, and the Ph.D. degree from the University of Montenegro in 1988, all in electrical engineering.

As a Fulbright grantee, he spent the 1984–1985 academic year at the Worcester Polytechnic Institute, Worcester, MA. Since 1982, he has been on the faculty at the University of Montenegro, where he has been a Full Professor since 1995. Since 2003, he has been the Rector of the University of Montenegro. He was also active in politics, as a Vice-President of the Republic of Montenegro from 1989 to 1991, and then as the leader of democratic (antiwar) opposition in Montenegro from 1991 to 1993. During 1997–1998 and 1999, he was on leave at the Ruhr University Bochum, Bochum, Germany, with Signal Theory Group, supported by the Alexander von Humboldt Foundation. At the beginning of 2001, he spent a period of time at the Technische Universiteit Eindhoven, Eindhoven, The Netherlands, as a visiting professor. From 2001 to 2002, he was the President of the Board of directors of the Montenegrin mobile phone company MONET. His current interests are in signal processing. He published about 270 technical papers, more than 80 of them in the leading international journals, mainly the IEEE editions. He has published several textbooks on signal processing (in Serbo-Croat) and the monograph *Time-frequency Signal Analysis* (in English).

Prof. Stanković received the "Best Student at the University" from the University of Montenegro. He also received the highest state award of the Republic of Montenegro in 1997 for scientific achievements. His group received a research grant for 2001 to 2003 from the Volkswagen Foundation, Federal Republic of Germany. He is a member the IEEE Signal Processing Society's Technical Committee on Theory and Methods, a member of the Yugoslav Engineering Academy, and a member of the National Academy of Science and Art of Montenegro (CANU). He is an Associate Editor of the IEEE TRANSACTIONS ON IMAGE PROCESSING and the IEEE SIGNAL PROCESSING LETTERS.

Thayananthan Thayaparan received the B.Sc. (Hons.) degree in physics from the University of Jaffna, Srilanka, in 1987, the M.Sc. degree in physics from the University of Oslo, Norway, in 1991, and the Ph.D. degree in atmospheric physics from the University of Western Ontario, Canada, in 1996.

From 1996 to 1997, he was a Postdoctoral Fellow at the University of Western Ontario. In 1997, he joined the Defence R&D Canada—Ottawa (DRDC Ottawa), Department of National Defence, Canada, as a Defence Scientist. He has published over 100 papers in international scientific journals and conferences. His research interests, *inter alia*, include time-frequency analysis, applications to radar signal and image processing, Inverse Synthetic Aperture Radar (ISAR), Synthetic Aperture Radar (SAR), Non-Cooperative Target Recognition (NCTR), Moving Target Detection (MTD), Automatic Target Recognition (ATR), meteors and ionosphere clutter in high-frequency (HF) radar, and winds and waves in the middle atmosphere using medium-frequency (MF) and very high-frequency (VHF) meteor radars.

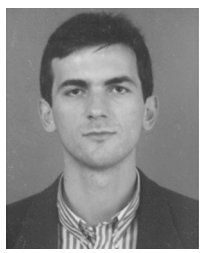

Miloš Daković was born in Nikšić, Montenegro, in 1970. He received the B.S., M.Sc., and Ph.D. degrees, all in electrical engineering, from the University of Montenegro in 1996, 2001, and 2005, respectively.

He is an Assistant Professor within the Electrical Engineering Department, University of Montenegro. His research interests are signal processing, time-frequency signal analysis, and radar signal processing. He is a member of the Time-Frequency Signal Analysis Group (www.tfsa.cg.yu) at the University of Montenegro, where he was involved in several research projects supported by Volkswagen Fondation, Montenegrian Ministry of Science and Canadian government (DRDC).